Differential Binding of Calmodulin Domains to Constitutive and Inducible Nitric Oxide Synthase Enzymes†

Donald E. Spratt, Valentina Taiakina, Michael Palmer, and J. Guy Guillemette*

Department of Chemistry, University of Waterloo, Waterloo, Ontario N2L 3G1, Canada

Received October 12, 2006; Revised Manuscript Received February 21, 2007

ABSTRACT: Calmodulin (CaM) is a Ca^{2+} signal transducing protein that binds and activates many cellular enzymes with physiological relevance, including the mammalian nitric oxide synthase (NOS) isozymes: endothelial NOS (eNOS), neuronal NOS (nNOS), and inducible NOS (iNOS). The mechanism of CaM binding and activation to the iNOS enzyme is poorly understood in part due to the strength of the bound complex and the difficulty of assessing the role played by regions outside of the CaM-binding domain. To further elucidate these processes, we have developed the methodology to investigate CaM binding to the iNOS holoenzyme and generate CaM mutant proteins selectively labeled with fluorescent dyes at specific residues in the N-terminal lobe, C-terminal lobe, or linker region of the protein. In the present study, an iNOS CaM coexpression system allowed for the investigation of CaM binding to the holoenzyme; three different mutant CaM proteins with cysteine substitutions at residues T34 (N-domain), K75 (central linker), and T110 (C-domain) were fluorescently labeled with acrylodan or Alexa Fluor 546 C_5-maleimide. These proteins were used to investigate the differential association of each region of CaM with the three NOS isoforms. We have also N-terminally labeled an iNOS CaM-binding domain peptide with dabsyl chloride in order to perform FRET studies between Alexa-labeled residues in the N- and C-terminal domains of CaM to determine CaM's orientation when associated to iNOS. Our FRET results show that CaM binds to the iNOS CaM-binding domain in an antiparallel orientation. Our steady-state fluorescence and circular dichroism studies show that both the N- and C-terminal EF hand pairs of CaM bind to the CaM-binding domain peptide of iNOS in a Ca^{2+}-independent manner; however, only the C-terminal domain showed large Ca^{2+}-dependent conformational changes when associated with the target sequence. Steady-state fluorescence showed that Alexa-labeled CaM proteins are capable of binding to holo-iNOS coexpressed with nCaM, but this complex is a transient species and can be displaced with the addition of excess CaM. Our results show that CaM does not bind to iNOS in a sequential manner as previously proposed for the nNOS enzyme. This investigation provides additional insight into why iNOS remains active even under basal levels of Ca^{2+} in the cell.

Calmodulin (CaM)[1] is a ubiquitous ∼17 kDa Ca^{2+}-binding cytosolic protein involved in the binding and regulation of over 300 target proteins (*1*, *2*). Due to its ability to bind and affect many different intracellular processes, such as various kinases and ion channels, there is significant interest in better understanding the structural and conformational basis of CaM's ability to bind and recognize target proteins (*3*, *4*).

CaM consists of two globular domains joined by a central linker region. Each globular domain of CaM contains an EF hand pair with the C-terminal EF hand pair having a 10-fold greater affinity for Ca^{2+} than the N-terminal EF hand pair (*5*). Previous studies involving the fluorescently labeled central linker of CaM have been performed to determine CaM's association and dissociation rates from myosin light chain kinase, calcineurin, and CaM kinase II (*6*−*8*). In the archetypical model of CaM binding to a target protein, the Ca^{2+}-replete CaM wraps its two domains around a single α-helical target peptide (*9*, *10*). However, other conformations of CaM when bound to target proteins have been discovered (*3*, *11*−*14*).

The nitric oxide synthase (NOS, EC 1.14.13.39) enzymes catalyze the production of nitric oxide (•NO), an important free radical involved in a large variety of cellular processes such as neurotransmission, vasodilation, and immune defense (*15*). There are three mammalian NOS isoforms: neuronal

†This work was supported by NSERC (Grant 183521).

* Corresponding author. Tel: 519-888-4567 ext 35954. Fax: 519-746-0435. E-mail: jguillem@sciborg.uwaterloo.ca.

[1] Abbreviations: Ca^{2+}, calcium ion; acrylodan, 6-acryloyl-2-(dimethylamino)naphthalene; Alexa Fluor 546, Alexa Fluor 546 C_5-maleimide; dabsyl chloride, 4-(dimethylamino)azobenzene-4′-sulfonyl chloride; CaM, calmodulin; CaM-T34C, CaM where threonine 34 is mutated to a cysteine; CaM-K75C, CaM where lysine 75 is mutated to a cysteine; CaM-T110C, CaM where threonine 110 is mutated to a cysteine; CaM-T34C-acr, CaM-T34C labeled with acrylodan; CaM-K75C-acr, CaM-K75C labeled with acrylodan; CaM-T110C-acr, CaM-T110C labeled with acrylodan; CaM-T34C-Alexa, CaM-T34C labeled with Alexa Fluor 546; CaM-K75C-Alexa, CaM-K75C labeled with Alexa Fluor 546; CaM-T110C-Alexa, CaM-T110C labeled with Alexa Fluor 546; nCaM, CaM residues 1−75; cCaM, CaM residues 76−148; NOS, nitric oxide synthase; •NO, nitric oxide; eNOS, endothelial NOS (NOSIII); iNOS, inducible NOS (NOSII); nNOS, neuronal NOS (NOSI); cNOS, constitutive NOS enzymes; NADPH, reduced nicotinamide adenine dinucleotide phosphate; FMN, flavin mononucleotide; FAD, flavin adenine dinucleotide; heme, protoporphyrin IX; H_4B, (6*R*,6*S*)-2-amino-4-hydroxy-6-(L-erythro-1,2-dihydroxypropyl)-5,6,7,8-tetrahydropteridine; FRET, fluorescence (Förster) resonance energy transfer; PCR, polymerase chain reaction; DTT, dithiothreitol; ESI-MS, electrospray ionization−mass spectrometry; QTOF, quadrupole time of flight; EDTA, (ethylenedinitrilo)tetraacetic acid.

10.1021/bi062130b CCC: $37.00
Published on Web 06/20/2007

NOS (nNOS), endothelial NOS (eNOS), and inducible NOS (iNOS). All three enzymes are homodimeric with each monomer consisting of an N-terminal oxygenase domain and a multidomain C-terminal reductase domain. The oxygenase domain contains binding sites for heme, tetrahydrobiopterin (H_4B), and the substrates L-arginine and molecular oxygen while the reductase domain binds FMN, FAD, and NADPH (*16*). A CaM-binding domain separates the oxygenase and reductase domains. The mechanism of how CaM binding facilitates electron transfer from NADPH to the heme is not fully understood and is not equivalent in all three NOS isoforms (*17*). At elevated Ca^{2+} concentrations, CaM binds to the constitutive NOS (cNOS) enzymes, nNOS and eNOS, enabling conformational changes in the reductase domains that facilitate electron transfer from NADPH though the reductase-associated flavins to the catalytic heme in the oxygenase domain (*18*−*21*). The X-ray structure of CaM bound to the CaM-binding domain of eNOS shows that CaM binds in an antiparallel fashion with the N-terminal domain of CaM binding to the N-type site closer to the C-terminus of eNOS which corresponds to the reductase domain, while the C-terminal domain of CaM binds to the C-type site closer to the N-terminus, corresponding to the oxygenase domain (*22*). In contrast to the cNOS enzymes, iNOS is transcriptionally regulated in vivo by cytokines and binds to CaM at basal levels of Ca^{2+}. The Ca^{2+}-independent activity of iNOS appears to result from the concerted interactions of CaM with both the oxygenase and reductase domains in addition to the canonical CaM-binding region (*23*). The orientation of CaM when bound to iNOS has previously been proposed to bind in a parallel fashion based on kinetic analysis (*24*); however, this model has yet to be proven.

While there have been several studies that demonstrate different regions of CaM are important for the binding and activation of the cNOS holoenzymes (*20*, *25*−*28*), very little has been reported on the binding and activation of the iNOS enzyme by CaM (*17*, *24*, *29*). In the present study, we employed three different mutant CaM proteins with single cysteine substitutions found in each region of CaM: CaM-T34C (N-domain), CaM-K75C (central linker), and CaM-T110C (C-domain). These cysteine CaM mutants were fluorescently labeled with acrylodan or Alexa Fluor 546 C_5-maleimide to monitor their binding to synthetic NOS CaM-binding domain peptides and the holo-NOS enzymes, respectively. The CaM-binding peptides and holoenzymes of all three mammalian NOS isoforms were utilized since studies involving uncommon CaM-target binding modes require the use of target elements that extend well outside of the typical CaM-binding region of the protein (*3*). This study was designed to use steady-state fluorescence and spectropolarimetry in the investigation of select regions of CaM when binding to the CaM-binding domain peptides and holoenzymes of the three mammalian NOS isozymes and to determine the orientation of CaM when bound to iNOS through the use of fluorescence resonance energy transfer (FRET).

EXPERIMENTAL PROCEDURES

Molecular Cloning of CaM. The QuikChange site-directed mutagenesis procedure (*30*) was used to convert the threonine codons at positions 34 and 110 to cysteines in the kanamycin-resistant pET9dCaM plasmid consisting of the pET9d vector (Novagen) carrying rat calmodulin (*17*). The forward and reverse primers for the T34C mutation incorporated a unique *Sac*I reporter cut site: wt-T34Cfr, 5′ CAATAACAACCAAGGAGCTCGGG*TGT*GTGATGC-GGTCTC 3′, and wt-T34Crv, 5′ GAGACCGCATCAC*A-CA*CCCGAGCTCCTTGGTTGTTATTG 3′. The forward and reverse primers for the T110C mutation involved the removal of a *Pml*I cut site: wt-T110Cfr, 5′ GCAGAGCT-TCGCCACGTTATG*TGT*AACCTTGGAGAGAAG 3′, and wt-T110Crv, 5′ CTTCTCTCCAAGGTT*ACA*CATAACGTG-GCGAAGCTCTGC 3′. The resulting pCaM-T34C and pCaM-T110C vectors were confirmed by DNA sequencing. The pCaM-K75C in the ampicillin-resistant pET23d vector (Novagen) was a generous gift from Dr. Neal Waxham (University of Texas Medical School at Houston, Houston, TX) (*7*).

CaM Protein Expression, Purification, and Fluorescent Labeling. Overnight cultures of BL21(DE3) *Escherichia coli* transformed with pCaM-T34C and pCaM-T110C were used to inoculate 2 × 1 L of Luria−Bertani (LB) media in 4 L flasks supplemented with 30 μg/mL kanamycin. BL21(DE3) pLysS *E. coli* transformed with pCaM-K75C grown to saturation overnight was used to inoculate 2 × 1 L of LB media supplemented with 100 μg/mL ampicillin and 30 μg/mL chloramphenicol. Cultures were grown at 37 °C, 200 rpm, to an OD_{600} of 0.6−0.8, induced with 500 μM IPTG, and harvested after 4 h of expression. Cells were harvested by centrifugation, flash frozen on dry ice, and stored at −80 °C. Cells were thawed on ice, resuspended in four volumes of 50 mM MOPS, pH 7.5, 100 mM KCl, 1 mM EDTA, and 1 mM DTT, and homogenized using an Avestin EmulsiFlex-C5 homogenizer (Ottawa, Ontario, Canada). The CaM proteins were purified using phenyl-sepharose chromatography as previously described (*31*) with the exception that the dialysis buffer contained 1 mM DTT. The CaM protein concentrations were determined using an ϵ_{277} of 3029 M^{-1} cm^{-1} for CaM saturated with Ca^{2+} (*32*) and were subsequently frozen in aliquots on dry ice and stored at −80 °C. Electrospray ionization−mass spectrometry (ESI-MS) was performed on the purified CaM proteins using a Micromass Q-Tof Ultima GLOBAL mass spectrometer (Manchester, U.K.) with an internal standard (*17*, *29*). The CaM samples were prepared by transferring the protein into water using a YM10 centrifugal filter device (Amicon) and then diluted using a 1:1 CH_3CN/water solution containing 0.2% formic acid to a concentration of approximately 20 μM. The samples were infused at 10 μL/min. Raw data (*m*/*z*) were processed using MaxEnt1 software to yield spectra on a true molecular mass scale.

CaM Protein Labeling with Acrylodan and Alexa Fluor 546 C_5-Maleimide. The CaM proteins were transferred into labeling buffer (50 mM Tris-HCl, pH 7.2, containing either 1 mM EDTA or 1 mM $CaCl_2$) by gel filtration using a Sephadex G-25 PD-10 column (Amersham Biosciences, Canada) in order to remove the excess reducing agent in the CaM sample, as previously described (*33*). Prior to labeling, the CaM proteins were tested with 5,5′-dithiobis(2-nitrobenzoic acid) (DTNB) purchased from Sigma (Oakville, Ontario, Canada) to ensure that the cysteine sulfhydryl side chains were completely reduced and sufficiently reactive for labeling with acrylodan and Alexa Fluor 546 C_5-maleimide (Molecular Probes, Eugene, OR). Using an $\epsilon_{412} = 13600$ M^{-1} cm^{-1},

the reactivities of the cysteine residues were determined to be completely reactive in the presence of Ca^{2+} and EDTA. Acrylodan and Alexa Fluor 546 C_5-maleimide were dissolved in *N*,*N*′-dimethylformamide and 50 mM Tris, pH 7.5, respectively, to a concentration of 20 mM. Either 100 μL of acrylodan or Alexa Fluor 546 solution was added to 1 mL of 100 μM CaM protein (1.67 mg/mL). For acrylodan, the mixture was allowed to react overnight at 10 °C with slow mixing, whereas with Alexa Fluor 546, the mixture was mixed slowly and allowed to react for 2 h at room temperature. The labeling reactions were quenched with the addition of either excess β-mercaptoethanol or dithiothreitol. Excess dye was removed by gel filtration using a PD-10 column preequilibrated with 50 mM HEPES, 1 mM EDTA, and 150 mM NaCl, pH 7.5. Exhaustive dialysis against 50 mM HEPES, 1 mM EDTA, and 150 mM NaCl, pH 7.5, was performed to ensure that all noncovalently linked dye was removed from the labeled CaM proteins, as previously described in other labeling studies (*8*, *34*). Labeling yields were determined from absorbance spectra on a Varian Cary UV−visible spectrophotometer (Varian, Mississauga, Ontario, Canada). The amount of covalently bound acrylodan was determined using an ϵ_{391} of 20000 M^{-1} cm^{-1} (Molecular Probes). Covalently linked Alexa Fluor 546 was determined with an ϵ_{554} of 93000 M^{-1} cm^{-1} (Molecular Probes). To determine the extent of labeling, the CaM proteins labeled with acrylodan or Alexa Fluor 546 were subjected to ESI-MS to ensure that only sulfhydryl-specific labeling occurred.

iNOS Peptide Labeling with Dabsyl Chloride. Two milligrams of lyophilized human iNOS CaM-binding domain peptide, RPKRR EIPLK VLVKA VLFAC MLMRK (residues 507−531 prepared by Sigma Genosys), was dissolved in 1 mL of dabsyl chloride labeling buffer consisting of 0.1 M $NaCO_3$, pH 7.1. A labeling buffer with a more neutral pH was used to ensure selective labeling of the N-terminus of the peptide as opposed to other primary amines found in the peptide, such as the numerous lysine residues. Dabsyl chloride was dissolved in *N*,*N*′-dimethylformamide to a concentration of 25 mM. One hundred microliters of dabsyl chloride solution was added to 1 mL of iNOS peptide (2 mg/mL), and the mixture was allowed to react for 1.5 h at 4 °C with slow mixing. The reaction mixture was then centrifuged for 5 min at 14000*g* to remove particulate from the sample. Due to the large size of the pellet, the pellet was solubilized in 95% (v/v) H_2O, 5% (v/v) CH_3CN, and 0.1% (v/v) TFA, incubated for 10 min at room temperature, and subsequently centrifuged to remove insoluble particles. The presence of peptide in the resolubilized supernatant was confirmed using the DC protein assay (Bio-Rad), based upon the Lowry method.

The dabsyl-labeled iNOS peptide was then purified by reverse-phase chromatography on an AKTApurifier System for Chromatography (Amersham Biosciences, Baie d'Urfe, Quebec, Canada) using a Delta-Pak C18 2 × 150 mm column (300 Å pore size, 5 μm particle size). The aqueous mobile phase consisted of 95% (v/v) H_2O, 5% (v/v) CH_3CN, and 0.1% (v/v) TFA while the organic mobile phase containing 95% (v/v) CH_3CN, 5% (v/v) H_2O, and 0.1% (v/v) TFA was used to elute the labeled iNOS peptide. After a 2 column volume wash with the aqueous phase, a linear gradient of the organic mobile phase (1.5%/min) was used to elute the labeled peptide from the column. Eluted peptide was detected at 215 and 254 nm while dabsyl chloride was monitored at 466 nm. Unlabeled peptide eluted at 63% organic mobile phase while the labeled peptide eluted at 72% organic mobile phase. Isolation of dabsyl-labeled iNOS peptide was confirmed by ESI-MS with only singly labeled species being observed. The concentration of dabsyl-iNOS peptide was determined using an ϵ_{466} = 33000 M^{-1} cm^{-1}.

NOS Enzyme Expression and Purification. Rat neuronal NOS and bovine endothelial NOS were expressed and purified as previously described (*17*, *29*, *31*) with the exception that these enzymes had an N-terminal polyhistidine tail cloned upstream from their respective start codons. Human iNOS carrying a deletion of the first 70 amino acids and an N-terminal polyhistidine tail was coexpressed with CaM or nCaM mutant protein in BL21(DE3) *E. coli*. This protein will henceforth be referred to as iNOS. Each NOS enzyme was purified using ammonium sulfate precipitation, metal chelation chromatography, and 2′,5′-ADP affinity chromatography as previously reported (*17*).

Enzyme Kinetics. The initial rate of •NO synthesis was measured using the spectrophotometric oxyhemoglobin capture assay as previously described (*31*). Assays were performed at 25 °C in a SpectraMax 384 Plus 96-well UV−visible spectrophotometer using Soft Max Pro software (Molecular Devices, Sunnyvale, CA). eNOS, nNOS, and iNOS coexpressed with CaM or nCaM (*17*) were assayed at concentrations of 70, 30, and 28.5 nM, respectively, in 100 μL total well volumes. Two hundred micromolar $CaCl_2$ or 250 μM EDTA as well as 2 μM wild-type CaM, mutant CaM protein, and labeled CaM proteins was added to the appropriate samples.

Steady-State Fluorescence. Fluorescence emission spectra were obtained using a PTI QuantaMaster spectrofluorometer (London, Ontario, Canada). CaM-T34C-acr, CaM-K75C-acr, or CaM-T110C-acr (100 nM) was used as the fluorescent reporter in the quartz cuvette, similar to a previous study involving calcineurin (*7*). The excitation wavelength for all of the acrylodan labeled CaMs was set at 375 nm. Slit widths were set at 2 nm for excitation and 2 nm for emission. In a volume of 1 mL, an initial scan was taken with each CaM-Cys-acr protein in a buffer consisting of 50 mM HEPES, 1 mM EDTA, and 150 mM NaCl, pH 7.5. After the first scan, synthetic NOS CaM-binding domain peptide (500 nM) was added to the cuvette, and the sample was mixed thoroughly, incubated for 3 min to allow the sample to reach equilibrium, and scanned. The calculated free $[Ca^{2+}]$ in this system is <1 nM based on calculations using the online algorithm WEBMAXC (*35*). The NOS CaM-binding domain peptide for human iNOS, RPKRR EIPLK VLVKA VLFAC MLMRK (residues 507−531), was prepared by Sigma Genosys, while bovine eNOS, TRKKT FKEVA NAVKI SASLM (residues 493−512), and rat nNOS, KRRAI GFKKL AEAVK FSAKL MGQ (residues 725−747), were synthesized by SynPeP (SynPeP Corp., Dublin, CA). The sample was then brought to a final free Ca^{2+} concentration calculated to be 0.500 mM, mixed, allowed to incubate for 3 min, and scanned. Finally, excess EDTA (5 mM final) was added (calculated free $[Ca^{2+}]$ of 5.8 nM), the sample was incubated for 3 min, and a final scan was taken.

Steady-state fluorescence measurements of CaM-Cys-Alexa Fluor 546 proteins (50 nM) binding to holo-NOS proteins (250 nM) were performed as previously described

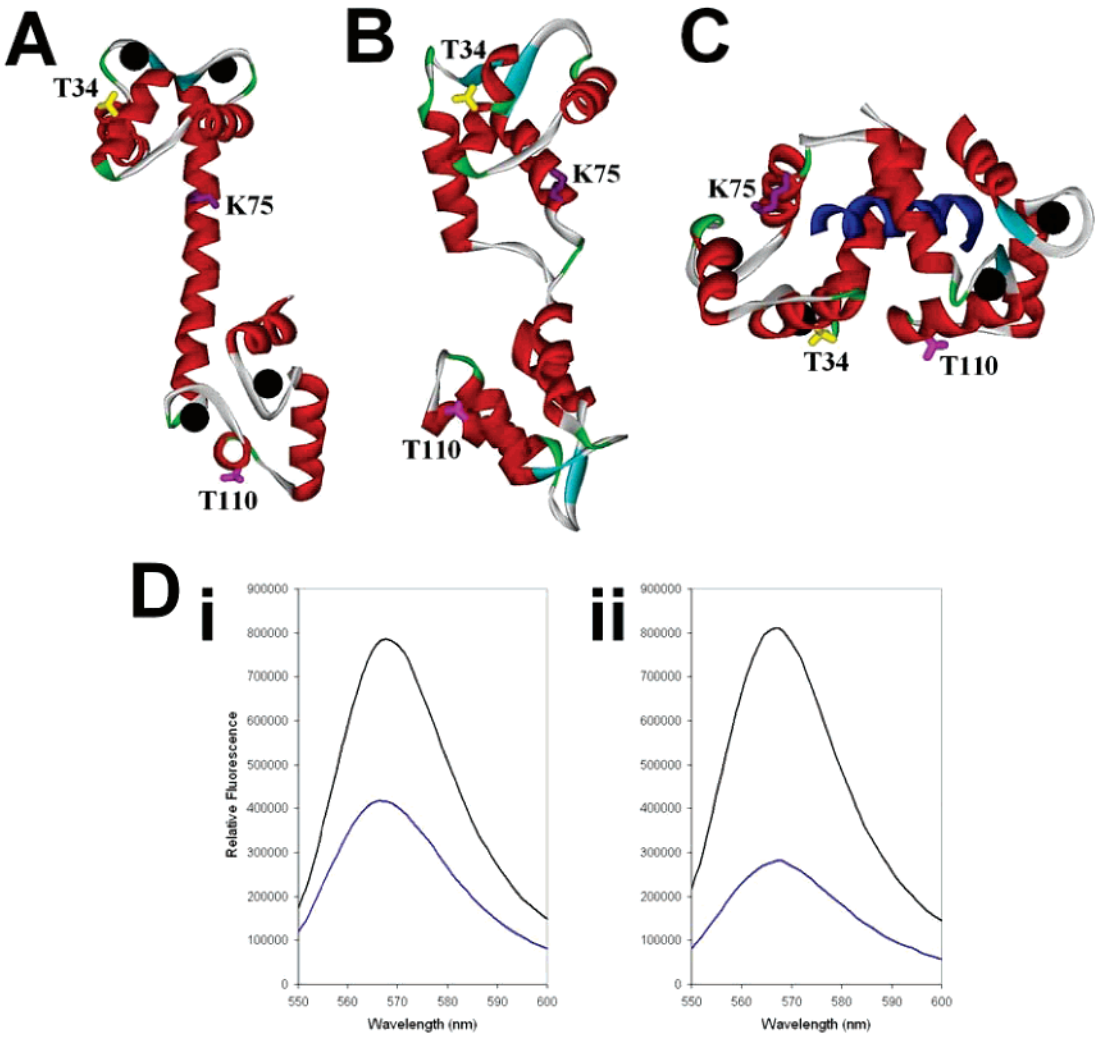

FIGURE 1: X-ray and NMR structures showing the positions of T34, K75, and T110 in (A) holo-CaM, (B) apo-CaM, and (C) CaM when bound to eNOS peptide. CaM, eNOS peptide, and Ca^{2+} ions are shown in red, blue, and black, respectively. T34, K75, and T110 are shown in yellow, purple, and pink, respectively. Models are derived from PDB codes 1CLL (*39*), 1CFD (*40*), and 1NIW (*22*). (D) FRET analysis of (i) CaM-T34C-Alexa and (ii) CaM-T110C-Alexa binding to iNOS peptide N-terminally labeled with dabsyl chloride. Alexa-labeled CaMs alone in the presence of Ca^{2+} and in the presence of dabsyl-iNOS peptide are shown as black and blue lines, respectively. The fluorescence signal of CaM-T110C-Alexa is quenched to a greater extent than CaM-T34C-Alexa when bound to the dabsyl-iNOS peptide.

(see above) with the exception that the excitation wavelength was set at 540 nm with emission monitored between 550 and 700 nm. The fluorescence emission maximum of Alexa-labeled CaM was observed at 567 nm, regardless of the presence of Ca^{2+} or EDTA in the buffer.

FRET Measurements of Alexa-Labeled CaMs with Dabsyl-Labeled iNOS Peptide. FRET measurements between dabsyl-labeled iNOS peptide and CaM-T34C-Alexa or CaM-T110C-Alexa were determined in a buffer consisting of 50 mM HEPES, 1 mM $CaCl_2$, and 150 mM NaCl, pH 7.5. Using the identical fluorometer setup as described for steady-state measurements with Alexa-labeled CaMs, an initial scan of 50 nM CaM-T34C-Alexa or CaM-T110C-Alexa alone in a volume of 1 mL was taken. This was followed by the addition of dabsyl-iNOS peptide, the sample was mixed well and incubated for 3 min, and a subsequent measurement was taken.

Circular Dichroism of nCaM or cCaM Bound to the Synthetic iNOS Peptide. Circular dichroism (CD) was performed in a Jasco J-715 CD spectropolarimeter using J-715 analysis software as previously described (*36*) with some modifications. Samples were measured in a 1 mm quartz cuvette (Hellma, Concord, Ontario, Canada) kept at 25 °C using a Peltier-type constant-temperature cell holder (model PFD 3505; Jasco, Easton, MD). Samples consisted of 25 μM nCaM or cCaM alone or equimolar concentrations of CaM protein with synthetic iNOS CaM-binding domain peptide. Samples were mixed in 10 mM Tris-HCl buffer (pH 7.5) containing 150 mM NaCl and 200 μM $CaCl_2$, followed by 1 mM EDTA. Spectra were recorded over a 190−250 nm range with a 1.0 nm bandwidth, 0.2 nm resolution, 100 mdeg sensitivity at a 0.125 s response, and a rate of 100 nm/min with a total of 25 accumulations. Data are expressed as the mean residue ellipticity (θ) in deg cm^2 $dmol^{-1}$.

RESULTS

Protein Expression, Purification, and Labeling. The CaM constructs used here have previously been employed in FRET and fluorescence binding studies with CaM target proteins due to their optimal positions in the N- and C-terminal domains (*37*, *38*), as well as the central linker of CaM (*7*, *8*) with all three CaM mutants showing no significant effect on enzyme activity. Figure 1 shows the positions of the mutant residues in the reported protein structures of holo-

Table 1: CaM-Cys and Fluorescently Labeled CaM-Dependent Activation of cNOS Enzymes[a]

CaM protein	neuronal NOS (%)	endothelial NOS (%)
CaM	100 ± 6	100 ± 1
CaM-T34C	114 ± 7	106 ± 5
CaM-T34C-acrylodan	238 ± 6[b]	87 ± 1
CaM-T34C-Alexa Fluor 546	156 ± 7[c]	104 ± 5
CaM-K75C	113 ± 3	116 ± 2
CaM-K75C-acrylodan	260 ± 7[b]	102 ± 2
CaM-K75C-Alexa Fluor 546	64 ± 4[c]	97 ± 5
CaM-T110C	89 ± 6	97 ± 2
CaM-T110C-acrylodan	157 ± 9[b]	116 ± 1
CaM-T110C-Alexa Fluor 546	185 ± 6[c]	93 ± 6
CaM (EDTA)	NAA[d]	NAA

[a] The oxyhemoglobin capture assay used to measure the rate of CaM-activated •NO production was performed in the presence of either 2 μM wild-type or mutant CaM protein and either 200 μM $CaCl_2$ or 250 μM EDTA, as indicated. The activities obtained with the respective enzyme bound to wild-type CaM at 25 °C in the presence of 200 μM $CaCl_2$ were all set to 100%. The activities for nNOS and eNOS bound to CaM were 35.4 and 9.5 min^{-1}, respectively. [b] Each assay that contained acrylodan-labeled CaM showed markedly greater activity than the equivalent CaM-Cys protein not labeled with acrylodan. [c] Alexa-CaMs showed increased activity when the N- and C-domains were labeled but displayed decreased activity when the central linker was labeled. [d] NAA, no apparent activity.

Table 2: CaM-Cys and Fluorescently Labeled CaM Activation of iNOS[a]

CaM protein	CaM protein added	inducible NOS (%)
iNOSwtCaM (Ca^{2+})	no	100 ± 2
iNOSnCaM (Ca^{2+})	no	64 ± 2
iNOSnCaM (EDTA)	no	NAA[b]
iNOSnCaM (EDTA)	CaM	61 ± 4
iNOSnCaM (EDTA)	CaM-T34C	60 ± 5
iNOSnCaM (EDTA)	CaM-T34C-acrylodan	63 ± 6
iNOSnCaM (EDTA)	CaM-T34C-Alexa Fluor 546	21 ± 1
iNOSnCaM (EDTA)	CaM-K75C	54 ± 2
iNOSnCaM (EDTA)	CaM-K75C-acrylodan	56 ± 2
iNOSnCaM (EDTA)	CaM-K75C-Alexa Fluor 546	26 ± 1
iNOSnCaM (EDTA)	CaM-T110C	56 ± 4
iNOSnCaM (EDTA)	CaM-T110C-acrylodan	85 ± 3
iNOSnCaM (EDTA)	CaM-T110C-Alexa Fluor 546	21 ± 2

[a] •NO synthesis rates were measured as described in Table 1 with 2 μM exogenous CaM protein added only to the assays indicated. Each assay was performed in the presence of either 200 μM $CaCl_2$ or 250 μM EDTA as shown. The activity obtained for iNOS coexpressed with CaM and assayed in the presence of 200 μM $CaCl_2$ at 25 °C was 50.5 min^{-1} and was set to 100%. [b] NAA, no apparent activity.

CaM (PDB code 1CLL; *39*), apo-CaM (PDB code 1CFD; *40*), and CaM in complex with eNOS peptide (PDB code 1NIW; *22*). When comparing the three structures in Figure 1A−C, these residues exhibit varying solvent exposure depending upon the target protein CaM binds to, making these sites optimal for fluorescence binding studies with fluorophores that are highly sensitive to their environment, such as acrylodan.

The mutant CaM proteins were successfully overexpressed in *E. coli*. After purification, we obtained 37.7, 31.0, and 39.3 mg of protein/L of media of CaM-T34C, CaM-K75C, and CaM-T110C, respectively. ESI-MS QTOF confirmed homogeneity and ruled out any posttranslational modification (see Supporting Information, Table S1).

Acrylodan fluorescence was measured exclusively in the presence of the NOS CaM-binding domain peptides. Alexa Fluor 546 C_5-maleimide (Molecular Probes) was used during FRET binding studies using the N-terminally dabsyl-labeled iNOS peptide as well as steady-state fluorescence binding studies with the holo-NOS enzymes due to its far-red-shifted excitation and emission spectra. This dye is also advantageous due to its ability to be specifically excited in the presence of the NOS cofactors (heme, FMN, and FAD), which absorb over most of the visible spectrum. Characterization of the fluorescently labeled CaM proteins is further discussed in the Supporting Information section.

NOS Activation by CaM-Cys and Fluorescently Labeled CaM Proteins. The oxyhemoglobin capture assay was employed to determine if the CaM-Cys and the fluorescently labeled CaM-Cys proteins were capable of binding and activating the holo-NOS enzymes. The eNOS and nNOS enzymes all exhibited approximately 100% activity in the presence of CaM-T34C, CaM-K75C, and CaM-T110C when compared to wild-type CaM (Table 1). The activation of eNOS by the acrylodan and Alexa Fluor 546-labeled CaM proteins was the same as observed for the unlabeled CaM-Cys proteins (Table 1). In contrast, when nNOS was assayed in the presence of the acrylodan-labeled CaM proteins, the •NO production rates were enhanced from 160% (for CaM-T110C-acr) up to 260% (for CaM-T34C-acr) of the rate obtained for wild-type CaM. This observation may be due to acrylodan's highly hydrophobic properties causing a nonspecific hydrophobic interaction between the CaM-Cys-acr proteins and nNOS. Similarly, when nNOS was assayed with CaM-T34C-Alexa and CaM-T110C-Alexa, •NO synthesis rates were also enhanced. The nNOS activity in the prescence of CaM-K75C-Alexa was decreased to approximately 60%, which may be due to the large Alexa dye disrupting the CaM central linker interaction with nNOS. It is noteworthy that all of the CaM-Cys and labeled CaM-Cys proteins required the presence of Ca^{2+} to activate the cNOS enzymes (results not shown). Clearly, all of the fluorescently labeled CaM-Cys mutants are able to bind and activate the cNOS enzymes, with nNOS showing marked increases in •NO production rates.

In order to monitor if the labeled and unlabeled CaM-Cys proteins were capable of activating iNOS, we used iNOS coexpressed with nCaM (CaM residues 1−75). In our previous study, we showed that iNOS coexpressed with nCaM displayed no apparent activity in the presence of EDTA; however, with the addition of 2 μM wild-type CaM with EDTA present, activity was maintained (*17*). This result indicated that a Ca^{2+}-dependent reorganization of the bound truncated nCaM mutant could facilitate its displacement and allow for the binding and activation of iNOS when excess native CaM is added. Significant levels of •NO synthesis were observed when excess CaM-Cys and CaM-Cys-acr mutants were added to iNOS coexpressed with nCaM in the presence of EDTA (Table 2). All of the mutant CaM proteins displayed identical activation profiles to that of iNOS coexpressed with nCaM with excess wild-type CaM (~60% maximal activation). The only exception was CaM-T110C-acr, which activated the enzyme to 85% maximal activity when compared to iNOS coexpressed with wild-type CaM (Table 2). This marked difference between CaM-T110C and its acrylodan-labeled equivalent may be due to a stronger hydrophobic interaction with iNOS, similar to the results previously observed with nNOS (Table 1). The Alexa Fluor

546-labeled CaM proteins showed low activation of iNOS (~20%), likely due to steric hindrance by the fluorophore (Table 2). Clearly, all of the acrylodan- and Alexa-labeled CaM proteins are capable of activating and, hence, binding to the iNOS enzyme in the absence of Ca^{2+}. The fact that the fluorescently labeled CaM proteins bind and activate the NOS isozymes indicates that the fluorescent binding studies we present in this study are relevant in describing CaM's association with the various NOS CaM-binding domains.

CaM−NOS Peptide Binding Studies. (A) FRET Studies Using Alexa-Labeled CaM Proteins with Dabsyl-Labeled iNOS Peptide. It has previously been shown that CaM binds to the CaM-binding domain of eNOS in an antiparallel fashion, meaning that the N-terminal domain of CaM binds closer to the C-terminus, classified as the N-type binding site, while the C-terminal domain of CaM binds closer to the N-terminus of the target protein, corresponding to the C-type binding site (*22*). It has also previously been determined that CaM binds to nNOS in an antiparallel orientation through NMR (*41*). Although it has previously been proposed that CaM binds to iNOS in a parallel orientation based upon kinetic data (*24*), this model has yet to be proven. In order to determine the orientation of CaM when bound to the CaM-binding domain of iNOS, we employed FRET to determine relative distances between the N- and C-domains from the N-terminus of an iNOS target peptide. CaM-T34C and CaM-T110C labeled with Alexa Fluor 546 were used as the FRET donors while a synthetic iNOS peptide N-terminally labeled with dabsyl chloride, which is a potent quencher, was used as the FRET acceptor. In essence, the greater the amount of quenching observed represents the Alexa-labeled site on CaM being closer to the N-terminus of the iNOS peptide. Should CaM-T34C-Alexa be quenched to a greater extent than CaM-T110C-Alexa, this would indicate that CaM binds in a parallel manner; however, if the reverse result is observed, this would represent that CaM binds to iNOS in an antiparallel fashion.

Our results shown in Figure 1D indicate that the fluorescence signal of CaM-T110C-Alexa is quenched to a greater extent than CaM-T34C-Alexa in the presence of dabsyl-iNOS peptide, signifying that when CaM is bound to the iNOS peptide, the C-domain of CaM is closer to the N-terminus of the peptide than the N-domain of CaM. This demonstrates that CaM does in fact bind to the iNOS CaM-binding domain in an antiparallel orientation, similar to that previously determined for the cNOS enzymes (*22*, *41*). The FRET results we obtained correlate well when compared to the published CaM−eNOS structure. This FRET donor−acceptor pair of Alexa Fluor 546 and dabsyl chloride has a theoretical Förster distance value (R_0) of 29 Å (Molecular Probes), which is optimal for measurements within this CaM−NOS peptide complex, based upon the solved CaM−eNOS structure (Figure 1C). The calculated distance between the hydroxyl moiety of T34 in CaM to the N-terminus of the eNOS peptide is 26.3 Å, while the distance between the hydroxyl of T110 to the N-terminus of the eNOS peptide is 19.2 Å. The fluorescence intensity of CaM-T34C-Alexa is approximately 50% when compared to its initial intensity without the dabsyl-iNOS peptide present, indicating that the fluorescence measurement is approximately equal to the R_0 value of 29 Å. This value is comparable to the measured distance between T34C and the N-terminus of the peptide in the CaM-eNOS structure, further supporting our finding that CaM binds to iNOS in an antiparallel fashion.

(B) Ca^{2+}-Dependent Association of Different Regions of CaM to the NOS Peptides. The binding of acrylodan-labeled CaM proteins to synthetic NOS CaM-binding domain peptides was observed using steady-state fluorescence. The addition of Ca^{2+} to the acrylodan-labeled CaM proteins all demonstrated marked changes in fluorescence intensity (Figure 2, Supporting Information). The addition of the eNOS and nNOS peptides caused little or no change in fluorescence emission of the CaM-T110C-acr protein in the presence of EDTA, signifying little or no interaction between the acrylodan-labeled CaMs and the cNOS peptides. In contrast, there was ~20% quenching when the iNOS peptide was added, indicative of an association between the peptide and CaM-T110C-acr (Figure 2A). The addition of Ca^{2+} resulted in a marked red shift and a fluorescence intensity decrease of CaM-T110C-acr in the presence of all three NOS peptides, indicating that the fluorophore becomes more solvent exposed upon CaM binding to the NOS peptides (Figure 2A). These large Ca^{2+}-dependent changes in acrylodan fluorescence with Ca^{2+} added are indicative of CaM binding to the cNOS peptides, while it represents a large Ca^{2+}-dependent conformational change in the C-domain of CaM when bound to the iNOS peptide. Finally, after the addition of excess EDTA, the acrylodan fluorescence signals closely returned to their original peaks prior to Ca^{2+} addition, signifying the release of the cNOS peptides from the acrylodan-labeled CaM proteins (Figure 2A). These results are consistent with the interaction of CaM with eNOS and nNOS being Ca^{2+}-dependent. While these results demonstrate that the C-domain of CaM does interact with the iNOS CaM-binding domain in a Ca^{2+}-independent manner, it is notable that this domain also experiences a large Ca^{2+}-dependent conformational change when it is associated with iNOS.

CaM-T34C-acr showed no change in fluorescence in the presence of EDTA, indicating no apparent interaction with the eNOS and nNOS peptides (Figure 2A). A marked blue shift in fluorescence emission was observed with the addition of Ca^{2+}, signifying that CaM-T34C-acr is associating with the cNOS peptides; however, the subsequent addition of EDTA caused the fluorescence signal to return to its original intensity, representing the release of CaM-T34C-acr from the cNOS peptides (Figure 2A). These observations further demonstrate that the association of the N-domain of CaM is Ca^{2+}-dependent when binding to the eNOS and nNOS peptides. In contrast, CaM-T34C-acr showed a blue shift upon addition of the iNOS peptide in the presence of EDTA (Figure 2A), indicating Ca^{2+}-independent binding. The subsequent addition of Ca^{2+} to the CaM-T34C-acr protein showed a slight red shift in emission, while the final addition of excess EDTA showed small changes in fluorescence intensity, but the spectra never returned to its original peak prior to the addition of iNOS peptide or Ca^{2+} (Figure 2A). These small changes in fluorescence are indicative of small structural rearrangements in the N-domain of CaM when associated with the iNOS peptide depending on the Ca^{2+} concentration rather than the release of the peptide. This is further exemplified in Figure 2B, where the addition of Ca^{2+} to CaM-T34C-acr alone results in a 5-fold increase in fluorescence with a large blue shift, indicative of the fluorophore moving into a more hydrophobic environment

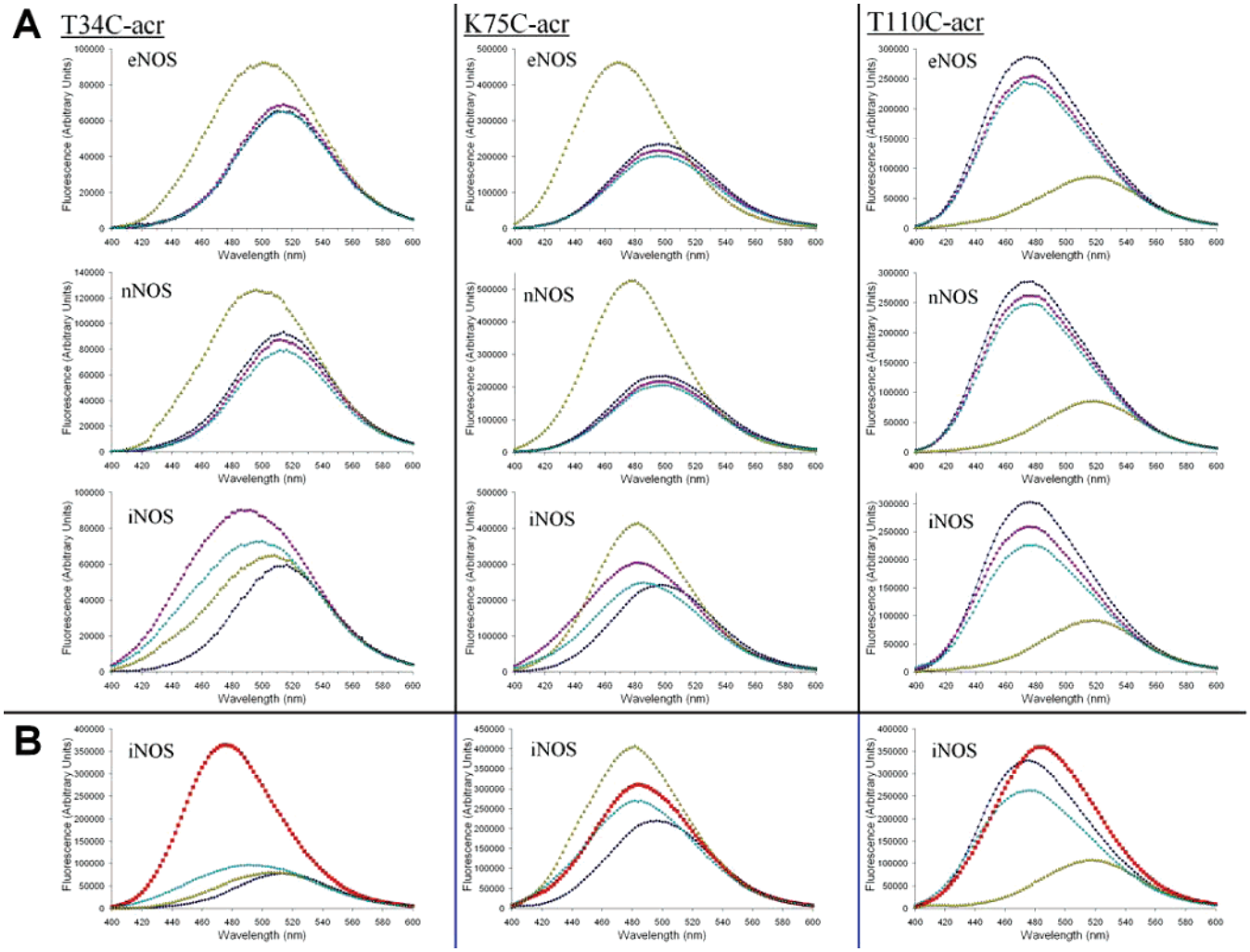

FIGURE 2: Steady-state fluorescence of CaM-Cys-acr proteins binding to synthetic NOS CaM-binding domain peptides. (A) In an initial volume of 1 mL, either CaM-T34C-acr, CaM-K75C-acr, and CaM-T110C-acr (100 nM final) was added to 50 mM HEPES, 150 mM NaCl, and 1 mM EDTA, pH 7.5, and the emission of each sample was observed between 400 and 600 nm (black diamonds). The excitation wavelength was set to 375 nm, and the excitation and emission slit widths were set at 2 nm. Synthetic NOS peptide (500 nM) was added to the aforementioned cuvette and mixed thoroughly, and another scan was taken (magenta squares). 1.5 mM $CaCl_2$ (0.5 mM final) was then added, and another scan was obtained (yellow triangles). In all cases, the addition of Ca^{2+} to the cuvette showed changes in the fluorescence emission signal and maxima. Lastly, EDTA was added to a final concentration of 5 mM, and an additional scan was taken (cyan circles). In between each addition, the sample was allowed to incubate for 3 min to reach equilibrium. (B) Conditions used were identical to those in (A) with the exception that $CaCl_2$ (0.5 mM) was added to the cuvette before the addition of any NOS peptide. The order of addition to the cuvette was as follows: (1) 100 nM CaM-Cys-acr in 1 mM EDTA (black diamonds), (2) $CaCl_2$ (0.5 mM final, red squares), (3) 500 nM iNOS peptide (yellow triangles), and finally (4) EDTA (5 mM final, cyan circles). Samples were incubated for 3 min between each measurement. These measurements were taken to ensure that the fluorescence spectra obtained in (A) for iNOS with each of the CaM-Cys-acr mutants were reproducible regardless of the order of Ca^{2+} or NOS peptide addition.

in a Ca^{2+}-dependent manner (Figure 2B). With the subsequent addition of the iNOS peptide, fluorescence is markedly attenuated, which could only result from CaM-T34C-acr's association to the iNOS peptide (Figure 2B). Furthermore, the fluorescence spectra after the addition of the iNOS peptide were identical for all of the acrylodan-labeled CaMs binding to the iNOS peptide in the presence of Ca^{2+} (Figure 2B) as was observed in Figure 2A, where the peptide was added to the cuvette before Ca^{2+}. Taken together, the fluorescence spectra obtained for acrylodan-labeled CaM in the presence of iNOS are reproducible regardless of the order of addition of either Ca^{2+} or the iNOS peptide (Figure 2). CaM binding to the iNOS peptide in the absence of Ca^{2+} was observable with CaM-T34C-acr, indicative of the fact that the Ca^{2+}-independent association previously observed with peptides derived from the CaM-binding domain of iNOS (*42*−*45*) may be predominantly due to the binding of the Ca^{2+}-depleted N-terminal lobe of CaM.

Fluorescence measurements of CaM's central linker with CaM-K75C-acr showed Ca^{2+} dependence when binding to the cNOS peptides (Figure 2A). This can be related to its position in the central linker of CaM between the two CaM domains that demonstrated a Ca^{2+}-dependent association to the eNOS and nNOS peptides (Figure 2A). In contrast, CaM-K75C-acr showed moderate Ca^{2+}-dependent changes in fluorescence likely due to some structural rearrangement in the presence of the iNOS peptide and EDTA (Figure 2). These fluorescent changes are most likely due to the C-terminal Ca^{2+}-dependent conformational changes when associated with the iNOS peptide. In summary, these steady-state fluorescence studies indicate that the N- and C-terminal domains of CaM bind to the iNOS peptide in a Ca^{2+}-

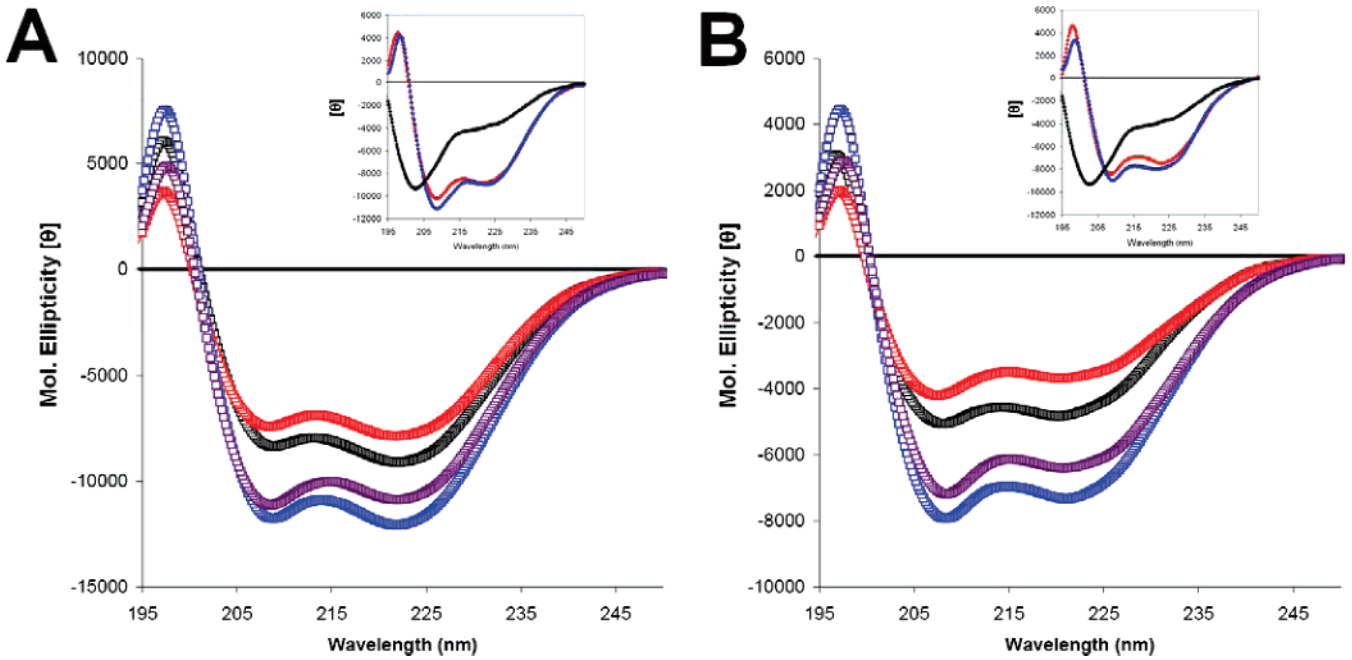

FIGURE 3: Effect of Ca^{2+} on the secondary structure of (A) nCaM and (B) cCaM bound to synthetic iNOS CaM-binding domain peptide. A spectropolarimetry study was performed on 25 μM nCaM (CaM residues 1−75) or cCaM (CaM residues 76−148) with and without 25 μM iNOS peptide. nCaM and cCaM proteins alone in the presence of 200 μM $CaCl_2$ or 1 mM EDTA are shown as black and red squares, respectively. nCaM or cCaM with iNOS peptide in the presence of 200 μM $CaCl_2$ or 1 mM EDTA are shown as cyan and magenta squares, respectively. Insets: The difference CD spectrum of the respective truncated CaM protein incubated with the iNOS peptide minus the corresponding spectrum of the CaM protein alone. Spectra were collected in the presence of either 200 μM Ca^{2+} (red diamonds) or 1 mM EDTA (blue diamonds). The CD spectrum of the iNOS peptide alone (black circles) is included for comparison.

independent manner. However, the N-domain of CaM demonstrated a lower susceptibility to Ca^{2+} concentrations as evidenced by minimal changes in conformation, while the C-terminal domain of CaM shows evidence of a Ca^{2+}-dependent rearrangement when associated with the iNOS peptide.

Our steady-state results for acrylodan-labeled CaM proteins binding to cNOS CaM-binding domain peptides are in good agreement with the degree of solvent exposure of these residues in the holo- and apo-CaM structures represented in Figure 1A−C. For T34, the residue is highly solvent exposed in the apo-CaM structure, almost completely exposed in holo-CaM, but more protected from solvent in the CaM−eNOS structure. K75 is relatively solvent exposed in the apo- and holo-CaM structures, whereas when CaM is bound to eNOS, this residue is more buried. Finally, T110 is relatively buried in the apo- and holo-CaM structures; conversely, T110 is more solvent exposed in the CaM−eNOS crystal structure.

The large change in fluorescence intensity upon peptide binding to Ca^{2+}-replete CaM-T110C-acr provided a means of determining the binding affinities of each of the peptides for CaM. Scans were taken between increasing molar ratios of peptide to CaM and repeated for various concentrations of CaM-T110C-acr (see Supporting Information, Figure S1 and Table S2). The affinities of the CaM-T110C-acr proteins for all three peptides were equivalent to previously reported binding studies that had used a variety of biophysical techniques as discussed in the Supporting Information section. These results are consistent with our observations that introduction of a fluorescent probe at this site still allowed for the binding and activation of the NOS holoenzymes.

(C) Effect of nCaM and cCaM on the Secondary Structure of the iNOS Peptide. We used circular dichroism (CD) to further investigate the interaction between the N- and C-lobes of CaM and the iNOS CaM-binding domain. Two previous investigations have shown that spectropolarimetry can be used to monitor the secondary structure of peptides that are bound to CaM (*42*, *43*). In order to obtain a CD spectrum for nCaM and cCaM when bound to the iNOS peptide, measurements were taken at 25 μM concentration (Figure 3). In the absence of nCaM or cCaM, the iNOS peptide showed no secondary structure and was predominantly random coil (Figure 3, inset). The binding of either Ca^{2+}-replete nCaM or cCaM to the iNOS peptide resulted in a large increase in α-helical content. Ca^{2+} chelation by EDTA resulted in a decrease in α-helical content of the complex (Figure 3). Further analysis using of the difference spectra in both experiments shows that the peptide retains some α-helical content when the iNOS peptide is in the presence of either apo-nCaM or apo-cCaM (Figure 3, inset). These results are consistent with published investigations of the binding of holo-apoCaM to the iNOS CaM-binding peptide (*42*, *43*). It is notable that both lobes can remain bound and induce α-helical structure upon the peptide under Ca^{2+}-depleted conditions. These results further support our steady-state fluorescence observations that the N- and C-domains of CaM associate with the iNOS peptide in a Ca^{2+}-independent fashion.

Holo-NOS Enzyme Studies. CaM-binding domain peptides provide a good model for CaM binding to a target protein; however, in order to obtain a true representation of CaM's interaction with the target protein in vitro and in vivo, measurements with the target holoenzyme are required. This is due to other regions outside of the CaM-binding element which may affect CaM's association to the target protein (*3*).

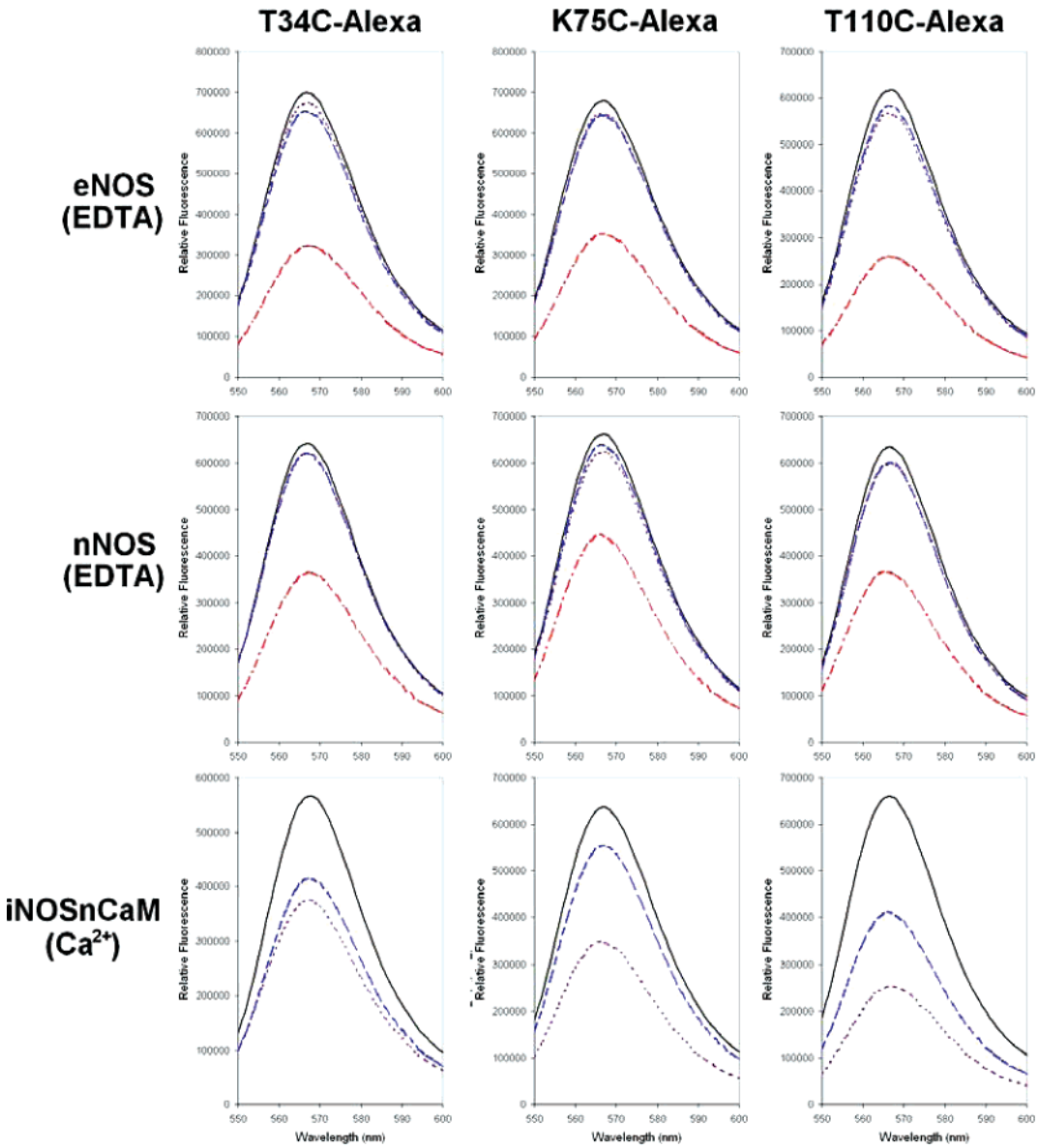

FIGURE 4: Steady-state fluorescence of Alexa Fluor 546 labeled CaM-Cys proteins binding to holo-NOS enzymes. In an initial volume of 1 mL, CaM-T34C-Alexa, CaM-K75C-Alexa, or CaM-T110C-Alexa (50 nM final) was added to 50 mM HEPES and 150 mM NaCl, pH 7.5. The initial scans of eNOS and nNOS contained 1 mM EDTA while scans with iNOS coexpressed with nCaM contained 1 mM $CaCl_2$. The excitation and emission slit widths were set at 2 nm. The excitation wavelength was set to 540 nm, and the emission of each sample was monitored between 550 and 600 nm (—). Holo-eNOS, nNOS, or iNOS coexpressed with nCaM (250 nM) was then added (— —), followed by 1.5 mM $CaCl_2$ (0.5 mM final) (— - —) and finally 5.5 mM EDTA (5 mM final) (- - -). In between each successive addition, individual scans were taken. Extra Ca^{2+} was not added to the samples containing iNOS coexpressed with nCaM because its initial scan already contained 1 mM $CaCl_2$.

(A) Alexa-CaM Binding to Holo-NOS Enzymes Using Steady-State Fluorescence. Prior to measuring CaM proteins associating with holo-NOS enzymes, control fluorescence measurements with Alexa-labeled CaM proteins with the NOS peptides were performed. As expected, no marked differences in fluorescence were observed, regardless of the presence of Ca^{2+} or EDTA, indicating that no quenching of the fluorophore emission occurs when bound to the NOS peptides (results not shown).

The CaM-Cys-Alexa proteins, which all emit at 567 nm, all showed a Ca^{2+}-dependent association to the eNOS and nNOS enzymes, as shown by quenching (Figure 4), as well as kinetic analysis (Table 1). This is apparent from the marked quenching of the fluorophore upon the addition of Ca^{2+} to the cuvette, most probably due to the dye being in close proximity to the heme cofactor since the heme shows broad absorbance over the entire visible spectrum, whereas FMN and FAD absorb very poorly in the 550−700 nm range (*46*).

We have previously used gel shift mobility assays to show that peptides coding for the CaM-binding domain of iNOS were capable of binding to two nCaM proteins, which consist of only the N-terminal EF hand pair of CaM (*17*). This indicated that nCaM was capable of binding to both the N-type and C-type binding regions of the iNOS CaM-binding peptide. The activity of iNOS coexpressed with nCaM was also shown to be Ca^{2+}-sensitive and the addition of excess wild-type CaM was able to activate the enzyme under Ca^{2+}-depleted conditions (Table 2; *17*). This was likely due to the replacement of nCaM from the C-type binding site by the C-terminal domain of wild-type CaM. Since the Alexa-labeled CaM proteins were also capable of activating the

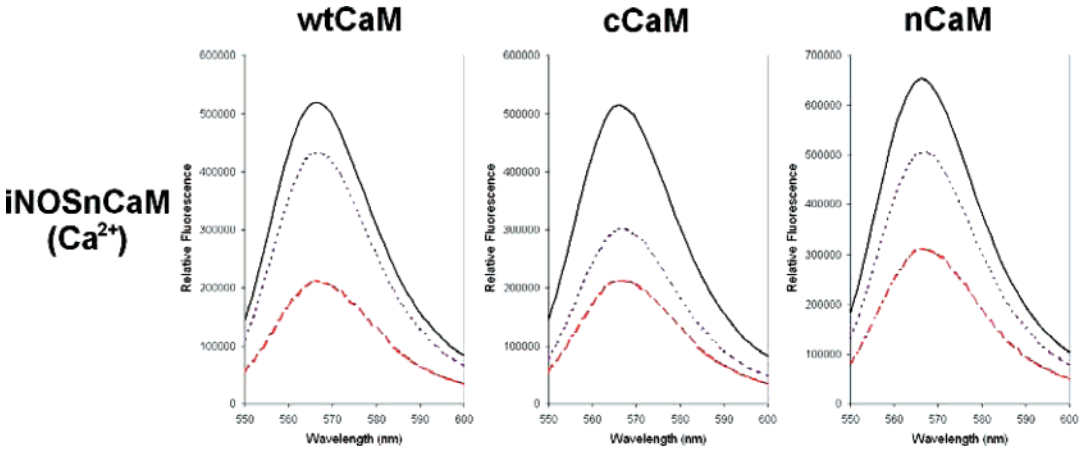

FIGURE 5: Dissociation of CaM-T110C-Alexa from iNOS coexpressed with nCaM after the addition of excess CaM proteins. An initial scan of CaM-T110C-Alexa in the presence of 1 mM $CaCl_2$ (—) was taken, followed by the addition of iNOS coexpressed with nCaM (250 nM) and EDTA to a final concentration of 5 mM (— - —). Once the sample reached equilibrium, a scan was taken, showing the quenched fluorescence due to the Alexa-labeled CaM binding to the iNOS enzyme. A 100-fold excess of unlabeled CaM protein was subsequently added, and scans were taken every minute until no further fluorescence increase was observed (- - -). Wild-type CaM, cCaM, and nCaM each took approximately 5 min, 15 min, and 2 h, respectively, to reach equilibrium.

iNOS coexpressed with nCaM in the presence of excess EDTA (Table 2), we concluded that the labeled CaMs were binding to the iNOS enzyme in a Ca^{2+}-independent manner. After the addition of iNOS coexpressed with nCaM to the Alexa-labeled CaMs, the samples were incubated for 5 min to allow the mixture to reach equilibrium. In each case, quenching of the fluorophore was observed, indicative of CaM associating to iNOS (Figure 4). CaM-T110C-Alexa showed the largest quenching effect, which can be attributed to the labeled residue binding directly to the C-type site being closest to the heme-containing oxygenase domain. This is in agreement with our FRET studies that show CaM binds to iNOS in an antiparallel fashion. The CaM-T34C-Alexa and CaM-K75C-Alexa showed smaller but similar trends in quenching (Figure 4). Upon the addition of EDTA to the cuvette, a greater quenching effect was observed for the CaM proteins labeled at residues 75 and 110, likely due to a Ca^{2+}-dependent conformational change in the C-terminus of the CaM protein that affects its interactions with iNOS (Figure 4). In contrast, CaM-T34C-Alexa showed almost no quenching upon the addition of EDTA (Figure 4) likely as a result of the N-domain of the labeled CaM failing to displace the coexpressed nCaM that is tightly bound to the N-type binding site of iNOS.

In contrast, we found that Alexa-CaM can displace nCaM from a dabsyl chloride-labeled iNOS CaM-binding domain (results not shown). Unlike the result we observed with holo-iNOS coexpressed with nCaM where nCaM remains bound to the N-type site of iNOS, both nCaMs that were bound to both the C- and N-type binding sites of the iNOS peptide are able to be completely displaced by CaM-T34C-Alexa and CaM-T110C-Alexa since their FRET measurements were identical to the data presented in Figure 1D. These results using the iNOS peptide further demonstrate why it is important to use holoenzymes when monitoring CaM binding to its target proteins because regions outside of the CaM-binding domain affect CaM's association. This is in agreement with a previous study that suggests both the CaM-binding domain and FMN domain of iNOS are required for the iNOS enzyme's Ca^{2+}-independent activity (*47*).

(B) Displacement of Alexa-CaM from iNOS by Addition of Excess CaM Proteins. Since CaM-T110C-Alexa showed Ca^{2+}-independent binding and the highest amount of fluorescence quenching when bound to iNOS, we tested if this binding of the C-terminal domain of CaM-T110C-Alexa was permanent or a transient species by the addition of excess CaM proteins under Ca^{2+}-depleted conditions. If the fluorescence signal increases, this would indicate that CaM-T110C-Alexa is released from the iNOS enzyme. Interestingly, fluorescence did increase upon the addition of a 100-fold excess (when compared to Alexa-CaM concentration) of wild-type CaM, cCaM, consisting of the central linker and C-terminal domain of CaM (residues 76−148), and nCaM, consisting of only the N-terminal domain of CaM with no central linker (residues 1−75) (Figure 5). This result indicated that the observed apo-CaM-T110C-Alexa association to the C-type binding site of iNOS is a transient species and can be replaced by another CaM protein. Although all of the excess CaM proteins were capable of out-competing CaM-T110C-Alexa, it is notable that the dissociation rates of the Alexa-labeled CaM were not equivalent. Wild-type CaM showed the quickest dissociation in approximately 5 min, followed by cCaM in 15 min (Figure 5). These proteins contain the C-terminal domain of CaM that normally interacts with the C-type binding site in the iNOS CaM-binding domain. In contrast, CaM-T110C-Alexa was displaced very slowly by excess nCaM, taking approximately 2 h to reach equilibrium (Figure 5). This result shows that the N-terminal lobe of CaM is capable of displacing CaM-T110C-Alexa from the C-type site; however, this dissociation is much slower, which can be attributed to apo-nCaM having a weak interaction with the C-type binding site. It is also important to note that this transient displacement of CaM-T110C-Alexa was only observed when excess CaM proteins were added to the sample: Chelation of Ca^{2+} alone was not sufficient to displace CaM-T110C-Alexa when bound to holo-iNOS.

DISCUSSION

The strong apparently Ca^{2+}-independent binding properties of CaM for the iNOS target sequence are quite remarkable, but this strong association has also made it difficult to

investigate. The solved structures of CaM in complex with peptides representing some of its target sequences have shown that CaM's association is predominantly in an antiparallel orientation (*9*, *10*, *14*, *22*, *48*−*51*) with the exception of IQ motifs, which bind in a parallel fashion (*52*, *53*). Recently reported structures of CaM bound to larger proteins that encompass its target sequences show the existence of additional novel modes of CaM binding (*11*−*14*, *54*−*57*). The ability of CaM to associate with these many and varied target proteins is not surprising due to CaM's highly flexible central linker which allows for the N- and C-lobes of CaM to obtain the most favorable conformation to bind with its target proteins. Both of the Ca^{2+}-dependent cNOS isoforms have been shown to bind in an antiparallel fashion (*22*, *41*). Surprisingly, a recent investigation had proposed that iNOS binds to CaM in a parallel orientation (*24*). This model would suggest that CaM may bind in a similar process to other Ca^{2+}-independent IQ motifs, such as neuromodulin; however, the CaM-binding domain of iNOS does not have any apparent homology to the IQ motifs. If this proposed model were true, it would have important implications for the interactions between CaM and iNOS. For this reason, we designed an experiment to determine the orientation of CaM binding to the iNOS peptide. We have found that CaM binds in an antiparallel fashion to iNOS, similar to that previously observed for the cNOS enzymes. Since the CaM-binding domains of the NOS enzymes show significant homology (*17*), our finding that CaM binds to iNOS in an antiparallel orientation is not surprising.

The use of short synthetic target peptides alone will not provide a full understanding of CaM binding and activation of target proteins (*3*). Previous observations have indicated that there are additional regions outside of the canonical CaM-binding domain that are important for the Ca^{2+}-independent binding of CaM to iNOS (*45*, *47*, *58*): To address this situation, we decided to use both an iNOS target peptide and the iNOS holoenzyme in our investigation of CaM binding and activation. The Ca^{2+} independence of CaM for iNOS has previously been attributed to favorable van der Waals contacts between the peptide and CaM and conformational changes to minimize unfavorable solvent exposure of the hydrophobic regions of the peptide (*22*). The exposure of hydrophobic regions of the iNOS CaM-target peptide upon complex formation has led to problems in aggregation (*43*), necessitating our use of a shorter iNOS CaM-target peptide and modified experimental procedures. A thorough investigation also necessitated the use of holoenzymes in our investigation: This required the purification of iNOS holoenzymes coexpressed in *E. coli* with either CaM or nCaM. We have previously demonstrated that iNOS can be coexpressed with the N-terminal domain of CaM alone to produce a stable and active enzyme (*17*). We further confirmed our previous study by demonstrating that the association of nCaM to the N-type binding site of the iNOS CaM-binding domain is very stable and does not appear to dissociate from holo-iNOS. This finding is supported by our steady-state fluorescence using holo-iNOS enzyme and Alexa-labeled CaMs, as well as our CD data monitoring the association between the iNOS CaM-binding peptide and the N- and C-lobes of CaM.

A sequential binding model consisting of the ordered binding of the C-terminal lobe to a C-type site followed by the binding of the N-terminal lobe to the N-type site has been proposed for various target proteins including nNOS (*59*). This mode of CaM association is consistent with the 10-fold higher affinity for Ca^{2+} in the C-lobe than the N-lobe of CaM (*5*) as well as the increased Ca^{2+} affinity when CaM is bound to its target sequence (*60*). At low basal levels of Ca^{2+}, the C-lobe of CaM is Ca^{2+}-replete and bound to the target sequence. As the cellular concentration of Ca^{2+} increases due to a signaling event, the N-lobe binds to Ca^{2+} allowing for its association with its target sequence leading to activation of the Ca^{2+}/CaM-dependent protein. We investigated the roles of different regions of CaM by using CaM proteins selectively labeled at three different residues. Notably, we showed that both CaM lobes are able to bind to iNOS in a Ca^{2+}-independent process. We were surprised to discover that the C-lobe, and not the N-lobe of CaM, showed the greatest Ca^{2+}-dependent changes in conformation when associated with either the iNOS peptide or the holoenzyme. Our results indicate that the aforementioned sequential model for nNOS does not necessarily apply to the Ca^{2+}-independent iNOS enzyme. This may be the case with iNOS where it has been shown that CaM's association and activation of iNOS is affected by the CaM-binding domain as well as other flanking regions of the enzyme (*45*, *47*, *58*).

Our results help to explain how iNOS remains active even under basal levels of Ca^{2+} in the cell. Unlike the cNOS enzymes, the N-terminal lobe of apo-CaM binds to the iNOS enzyme and retains activity, consistent with our previous study (*17*). We have also performed stopped-flow experiments using acrylodan-labeled CaM that show the iNOS peptide binds to CaM five times faster than the eNOS peptide (results not shown). In the cell where the number of CaM-binding proteins exceeds the amount of CaM present (*61*, *62*), the ability of iNOS to rapidly bind to CaM in a Ca^{2+}-independent manner is required to prevent aggregation of the enzyme (*63*). Although the structural basis for how these enzymes are bound and activated by CaM is not fully understood, our results further demonstrate that there are marked differences between the Ca^{2+}-dependent and -independent NOS isozymes in terms of their regulation by CaM.

ACKNOWLEDGMENT

We thank Dr. Neal Waxham (University of Texas Medical School at Houston) for generously providing the plasmid coding for CaM-K75C, Dr. Art Szabo (Wilfrid Laurier University) for providing the synthetic NOS CaM-binding domain peptides, and the reviewers for helpful suggestions for our manuscript.

SUPPORTING INFORMATION AVAILABLE

Supplemental materials and methods as described in the text. This material is available free of charge via the Internet at http://pubs.acs.org.

REFERENCES

1. Crivici, A., and Ikura, M. (1995) Molecular and structural basis of target recognition by calmodulin, *Annu. Rev. Biophys. Biomol. Struct. 24*, 85−116.
2. Ikura, M., and Ames, J. B. (2006) Genetic polymorphism and protein conformational plasticity in the calmodulin superfamily:

two ways to promote multifunctionality, *Proc. Natl. Acad. Sci. U.S.A. 103*, 1159−1164.
3. Ishida, H., and Vogel, H. J. (2006) Protein-peptide interaction studies demonstrate the versatility of calmodulin target protein binding, *Protein Pept. Lett. 13*, 455−465.
4. Bhattacharya, S., Bunick, C. G., and Chazin, W. J. (2004) Target selectivity in EF-hand calcium binding proteins, *Biochim Biophys. Acta 1742*, 69−79.
5. Martin, S. R., Anderson Teleman, A., Bayley, P. M., Drakenburg, T., and Forsen, S. (1985) Kinetics of calcium dissociation from calmodulin and its tryptic fragments. A stopped-flow fluorescence study using Quin 2 reveals a two-domain structure, *Eur. J. Biochem. 151*, 543−550.
6. Torok, K., and Trentham, D. R. (1994) Mechanism of 2-chloro-(ϵ-amino-Lys75)-[6-[4-(*N*,*N*-diethylamino)phenyl]-1,3,5-triazin-4-yl]calmodulin interactions with smooth muscle myosin light chain kinase and derived peptides, *Biochemistry 33*, 12807−12820.
7. Quintana, A. R., Wang, D., Forbes, J. E., and Waxham, M. N. (2005) Kinetics of calmodulin binding to calcineurin, *Biochem. Biophys. Res. Commun. 334*, 674−680.
8. Waxham, M. N., Tsai, A. L., and Putkey, J. A. (1998) A mechanism for calmodulin (CaM) trapping by CaM-kinase II defined by a family of CaM-binding peptides, *J. Biol. Chem. 273*, 17579−17584.
9. Meador, W. E., Means, A. R., and Quiocho, F. A. (1992) Target enzyme recognition by calmodulin: 2.4 Å structure of a calmodulin-peptide complex, *Science 257*, 1251−1255.
10. Ikura, M., Clore, G. M., Gronenborn, A. M., Zhu, G., Klee, C. B., and Bax, A. (1992) Solution structure of a calmodulin-target peptide complex by multidimensional NMR, *Science 256*, 632−638.
11. Drum, C. L., Yan, S. Z., Bard, J., Shen, Y. Q., Lu, D., Soelaiman, S., Grabarek, Z., Bohm, A., and Tang, W. J. (2002) Structural basis for the activation of anthrax adenylyl cyclase exotoxin by calmodulin, *Nature 415*, 396−402.
12. Schumacher, M. A. R. R. A., Bachinger, H. P., and Adelman, J. P. (2001) Structure of the gating domain of a Ca^{2+}-activated K^+ channel complexed with Ca^{2+}/calmodulin, *Nature 410*, 1120−1124.
13. Yap, K. L., Yuan, T., Mal, T. K., Vogel, H. J., and Ikura, M. (2003) Structural basis for simultaneous binding of two carboxy-terminal peptides of plant glutamate decarboxylase to calmodulin, *J. Mol. Biol. 328*, 193−204.
14. Ye, Q., Li, X., Wong, A., Wei, Q., and Jia, Z. (2006) Structure of calmodulin bound to a calcineurin peptide: a new way of making an old binding mode, *Biochemistry 45*, 738−745.
15. Alderton, W. K., Cooper, C. E., and Knowles, R. G. (2001) Nitric oxide synthases: structure, function and inhibition, *Biochem. J. 357*, 593−615.
16. Roman, L. J., Martásek, P., and Masters, B. S. (2002) Intrinsic and extrinsic modulation of nitric oxide synthase activity, *Chem. Rev. 120*, 1179−1190.
17. Spratt, D. E., Newman, E., Mosher, J., Ghosh, D. K., Salerno, J. C., and Guillemette, J. G. (2006) Binding and activation of nitric oxide synthase isozymes by calmodulin EF hand pairs, *FEBS J. 273*, 1759−1771.
18. Abu-Soud, H. M., Yoho, L. L., and Stuehr, D. J. (1994) Calmodulin controls neuronal nitric-oxide synthase by a dual mechanism. Activation of intra- and interdomain electron transfer, *J. Biol. Chem. 269*, 1179−1190.
19. Chen, P. F., Tsai, A. L., Berka, V., and Wu, K. K. (1996) Endothelial nitric-oxide synthase. Evidence for bidomain structure and successful reconstitution of catalytic activity from two separate domains generated by a baculovirus expression system, *J. Biol. Chem. 271*, 14631−14635.
20. Stevens-Truss, R., Beckingham, K., and Marletta, M. A. (1997) Calcium binding sites of calmodulin and electron transfer by neuronal nitric oxide synthase, *Biochemistry 36*, 12337−12345.
21. Ghosh, D. K., and Salerno, J. C. (2003) Nitric oxide synthases: domain structure and alignment in enzyme function and control, *Front. Biosci. 8*, 193−209.
22. Aoyagi, M., Arvai, A. S., Tainer, J. A., and Getzoff, E. D. (2003) Structural basis for endothelial nitric oxide synthase binding to calmodulin, *EMBO J. 22*, 766−775.
23. Lee, S. J., and Stull, J. T. (1998) Calmodulin-dependent regulation of inducible and neuronal nitric-oxide synthase, *J. Biol. Chem. 273*, 27430−27437.
24. Gribovskaja, I., Brownlow, K. C., Dennis, S. J., Rosko, A. J., Marletta, M. A., and Stevens-Truss, R. (2005) Calcium-binding sites of calmodulin and electron transfer by inducible nitric oxide synthase, *Biochemistry 44*, 7593−7601.
25. Persechini, A., Gansz, K. J., and Paresi, R. J. (1996) Activation of myosin light chain kinase and nitric oxide synthase activities by engineered calmodulins with duplicated or exchanged EF hand pairs, *Biochemistry 35*, 224−228.
26. Persechini, A., Gansz, K. J., and Paresi, R. J. (1996) A role in enzyme activation for the N-terminal leader sequence in calmodulin, *J. Biol. Chem. 271*, 19279−19282.
27. Gachhui, R., Abu-Soud, H. M., Ghosh, D. K., Presta, A., Blasing, M. A., Mayer, B., George, S. E., and Stuehr, D. J. (1998) Neuronal nitric-oxide synthase interaction with calmodulin-troponin C chimeras, *J. Biol. Chem. 273*, 5451−5454.
28. Su, Z., Blazing, M. A., Fan, D., and George, S. E. (1995) The calmodulin-nitric oxide synthase interaction. Critical role of the calmodulin latch domain in enzyme activation, *J. Biol. Chem. 270*, 29117−29122.
29. Newman, E., Spratt, D. E., Mosher, J., Cheyne, B., Montgomery, H. J., Wilson, D. L., Weinburg, J. B., Smith, S. M. E., Salerno, J. C., Ghosh, D. K., and Guillemette, J. G. (2004) Differential activation of nitric-oxide synthase isozymes by calmodulin-troponin C chimeras, *J. Biol. Chem. 279*, 33547−33557.
30. Wang, W., and Malcolm, B. A. (1999) Two-stage PCR protocol allowing introduction of multiple mutations, deletions and insertions using QuikChange site-directed mutagenesis, *BioTechniques 26*, 680−682.
31. Montgomery, H. J., Bartlett, R., Perdicakis, B., Jervis, E., Squier, T. C., and Guillemette, J. G. (2003) Activation of constitutive nitric oxide synthases by oxidized calmodulin mutants, *Biochemistry 42*, 7759−7768.
32. Gao, J., Yin, D., Yao, Y., Williams, T. D., and Squier, T. C. (1998) Progressive decline in the ability of calmodulin isolated from aged brain to activate the plasma membrane Ca-ATPase, *Biochemistry 37*, 9536−9548.
33. Lang, S., Spratt, D. E., Guillemette, J. G., and Palmer, M. (2005) Dual-targeted labeling of proteins using cysteine and selenomethionine residues, *Anal. Biochem. 342*, 271−279.
34. Ottl, J., Gabriel, D., and Marriott, G. (1998) Preparation and photoactivation of caged fluorophores and caged proteins using a new class of heterobifunctional, photocleavable cross-linking reagents, *Bioconjugate Chem. 9*, 143−151.
35. Patton, C., Thompson, S., and Epel, D. (2004) Some precautions in using chelators to buffer metals in biological solutions, *Cell Calcium 35*, 427−431.
36. Fernando, P., Abdulle, R., Mohindra, A., Guillemette, J. G., and Heikkila, J. J. (2002) Mutation or deletion of the C-terminal tail affects the function and structure of *Xenopus laevis* small heat shock protein, hsp30, *Comp. Biochem. Physiol., Part B: Biochem. Mol. Biol. 133*, 95−103.
37. Drum, C. L., Yan, S. Z., Sarac, R., Mabuchi, Y., Beckingham, K., Bohm, A., Grabarek, Z., and Tang, W. J. (2000) An extended conformation of calmodulin induces interactions between structural domains of adenylyl cyclase from *Bacillus anthracis* to promote catalysis, *J. Biol. Chem. 275*, 36334−36340.
38. Allen, M. W., Urbauer, R. J., Zaidi, A., Williams, T. D., Urbauer, J. L., and Johnson, C. K. (2004) Fluorescence labeling, purification, and immobilization of a double cysteine mutant calmodulin fusion protein for single-molecule experiments, *Anal. Biochem. 325*, 273−284.
39. Chattopadhyaya, R., Meador, W. E., Means, A. R., and Quiocho, F. A. (1992) Calmodulin structure refined at 1.7 Å resolution, *J. Mol. Biol. 228*, 1177−1192.
40. Kuboniwa, H., Tjandra, N., Grzesiek, S., Ren, H., Klee, C. B., and Bax, A. (1995) Solution structure of calcium-free calmodulin, *Nat. Struct. Biol. 2*, 768−776.
41. Zhang, M., Yuan, T., Aramini, J. M., and Vogel, H. J. (1995) Interaction of calmodulin with its binding domain of rat cerebellar nitric oxide synthase: A multinuclear NMR study, *J. Biol. Chem. 270*, 20901−20907.
42. Yuan, T., Vogel, H. J., Sutherland, C., and Walsh, M. P. (1998) Characterization of the Ca^{2+}-dependent and -independent interactions between calmodulin and its binding domain of inducible nitric oxide synthase, *FEBS Lett. 431*, 210−214.
43. Matsubara, M., Hayashi, N., Titani, K., and Taniguchi, H. (1997) Circular dichroism and ^{1}H NMR studies on the structures of peptides derived from the calmodulin-binding domains of inducible and endothelial nitric-oxide synthase in solution and in complex with calmodulin, *J. Biol. Chem. 272*, 23050−23056.

44. Zoche, M., Bienert, M., Beyermann, M., and Koch, K. W. (1996) Distinct molecular recognition of calmodulin-binding sites in the neuronal and macrophage nitric oxide synthases: a surface plasmon resonance study, *Biochemistry 35*, 8742−8747.
45. Anagli, J., Hormann, F., Quadroni, M., Vorherr, T., and Carafoli, E. (1995) The calmodulin-binding domain of the inducible (macrophage) nitric oxide synthase, *Eur. J. Biochem. 233*, 701−708.
46. Munro, A. W., and Noble, M. A. (1999) Fluorescence Analysis of Flavoproteins, in *Flavoprotein Protocols: Methods in Molecular Biology* (Chapman, S. K., and Reid, G. A., Eds.) Vol. 131, pp 25−48, Humana Press, Totowa, NJ.
47. Ruan, J., Wie, Q., Hutchinson, N., Cho, H., Wolfe, G. C., and Nathan, C. (1996) Inducible nitric oxide synthase requires both the canonical calmodulin-binding domain and addition sequences in order to bind calmodulin and produce nitric oxide in the absence of free Ca^{2+}, *J. Biol. Chem. 271*, 22679−22686.
48. Simonovic, M., Zhang, Z., Cianci, C. D., Steitz, T. A., and Morrow, J. S. (2006) Structure of the calmodulin alphaII-spectrin complex provides insight into the regulation of cell plasticity, *J. Biol. Chem. 281*, 34333−34340.
49. Maximciuc, A. A., Putkey, J. A., Shamoo, Y., and Mackenzie, K. R. (2006) Complex of calmodulin with a ryanodine receptor target reveals a novel, flexible binding mode, *Structure 14*, 1547−1556.
50. Contessa, G. M., Orsale, M., Melino, S., Torre, V., Paci, M., Desideri, A., and Cicero, D. O. (2005) Structure of calmodulin complexed with an olfactory CNG channel fragment and role of the central linker: residual dipolar couplings to evaluate calmodulin binding modes outside the kinase family, *J. Biomol. NMR 31*, 185−199.
51. Clapperton, J. A., Martin, S. R., Smerdon, S. J., Gamblin, S. J., and Bayley, P. M. (2002) Structure of the complex of calmodulin with the target sequence of calmodulin-dependent protein kinase I: studies of the kinase activation mechanism, *Biochemistry 41*, 14669−14679.
52. Fallon, J. L., Halling, D. B., Hamilton, S. L., and Quiocho, F. A. (2005) Structure of calmodulin bound to the hydrophobic IQ domain of the cardiac Ca(v)1.2 calcium channel, *Structure 23*, 1881−1886.
53. van Petegem, F., Chatelain, F. C., and Minor, D. L., Jr. (2005) Insights into voltage-gated calcium channel regulation from the structure of the CaV1.2 IQ domain-Ca^{2+}/calmodulin complex, *Nat. Struct. Mol. Biol. 12*, 1108−1115.
54. Kurokawa, H., Osawa, M., Kurihara, H., Katayama, N., Tokumitsu, H., Swindells, M. B., Kainosho, M., and Ikura, M. (2005) Target-induced conformational adaptation of calmodulin revealed by the crystal structure of a complex with nematode Ca^{2+}/calmodulin-dependent kinase kinase peptide, *J. Mol. Biol. 312*, 59−68.
55. Matsubara, M., Nakatsu, T., Kato, H., and Taniguchi, H. (2004) Crystal structure of a myristoylated CAP-23/NAP-22 N-terminal domain complexed with Ca^{2+}/calmodulin, *EMBO J. 23*, 712−718.
56. Yamauchi, E., Nakatsu, T., Matsubara, M., Kato, H., and Taniguchi, H. (2003) Crystal structure of a MARCKS peptide containing the calmodulin-binding domain in complex with Ca^{2+}-calmodulin, *Nat. Struct. Biol. 10*, 226−231.
57. Elshorst, B., Hennig, M., Forsterling, H., Diener, A., Maurer, M., Schulte, P., Schwalbe, H., Griesinger, C., Krebs, J., Schmid, H., Vorherr, T., and Carafoli, E. (1999) NMR solution structure of a complex of calmodulin with a binding peptide of the Ca^{2+} pump, *Biochemistry 38*, 12320−12332.
58. Venema, R. C., Sayegh, H. S., Kent, J. D., and Harrison, D. G. (1996) Identification, characterization, and comparison of the calmodulin-binding domains of the endothelial and inducible nitric oxide synthases, *J. Biol. Chem. 271*, 6435−6440.
59. Persechini, A., McMillan, K., and Leakey, P. (1994) Activation of myosin light chain kinase and nitric oxide synthase activities by calmodulin fragments, *J. Biol. Chem. 269*, 16148−16154.
60. Olwin, B. B., and Storm, D. R. (1985) Calcium binding to complexes of calmodulin and calmodulin binding proteins, *Biochemistry 24*, 8081−8086.
61. Tran, Q. K., Black, D. J., and Persechini, A. (2005) Dominant affectors in the calmodulin network shape the time courses of target responses in the cell, *Cell Calcium 37*, 541−553.
62. Persechini, A., and Stemmer, P. M. (2002) Calmodulin is a limiting factor in the cell, *Trends Cardiovasc. Med. 12*, 32−37.
63. Kolodziejska, K. E., Burns, A. R., Moore, R. H., Stenoien, D. L., and Eissa, N. T. (2005) Regulation of inducible nitric oxide synthase by aggresome formation, *Proc. Natl. Acad. Sci. U.S.A. 102*, 4854−4859.

BI062130B